PERGAMON

International Journal of Heat and Mass Transfer 45 (2002) 3849–3856

International Journal of HEAT and MASS TRANSFER

www.elsevier.com/locate/ijhmt

Field synergy principle for enhancing convective heat transfer—its extension and numerical verifications

Wen-Quan Tao [a,*], Zeng-Yuan Guo [b], Bu-Xuan Wang [b]

[a] School of Energy and Power Engineering, Xi'an Jiaotong University, Shaanxi, Xi'an 710049, China
[b] Tsinghua University, Beijing 100084, China

Received 28 December 2001

Abstract

The concept of enhancing parabolic convective heat transfer by reducing the intersection angle between velocity and temperature gradient is reviewed and extended to elliptic fluid flow and heat transfer situation. Five examples of elliptic flow are provided to show the validity of the new concept (field synergy principle). Two further examples are supplemented to demonstrate the importance of the concept in the design of the enhanced surfaces. © 2002 Published by Elsevier Science Ltd.

1. Introduction

The enhancement of convective heat transfer is an everlasting subject for both the researchers of heat transfer community of academia and the technicians in industry. Numerous investigations, both experimental and numerical have been conducted and great achievements have been obtained [1–5]. However, there is no unified theory which can reveal the essence of heat transfer enhancement common to all enhancement methods. In 1998, Guo and his co-workers proposed a novel concept for enhancing convective heat transfer of parabolic flow [6,7], the reduction of the intersection angle between velocity and temperature gradient can effectively enhance convective heat transfer. The purpose of this paper are threefold: the major idea of this novel concept will be extended to the general elliptic fluid flow and heat transfer; the numerical example will be provided to show the correctness of this new idea; and some examples of application will be provided to show the importance of this new concept.

Guos' proposal [6,7] will be briefly reviewed here. For two-dimensional (2-D) boundary layer flow and heat transfer along a plate with a temperature different from the oncoming flow, the energy equation takes following form:

$$\rho c_p\left(u\frac{\partial T}{\partial x}+v\frac{\partial T}{\partial y}\right)=\frac{\partial}{\partial y}\left(k\frac{\partial T}{\partial y}\right) \tag{1}$$

Integrating above equation along the thermal boundary layer and notice that at the outer edge of the thermal boundary layer $(\partial T/\partial y)_{y=\delta_t}=0$, we have

$$\rho c_p\int_0^{\delta_t}(\vec{U}\cdot\operatorname{grad}T)\,\mathrm{d}y=-\left(k\frac{\partial T}{\partial y}\right)_{y=0}=q_w \tag{2}$$

The convective term has been transformed to the dot product form of the velocity vector and the temperature gradient, and the right-hand side is the heat flux between the solid wall and the fluid, i.e., the convective heat transfer rate. The dot product $(\vec{U}\cdot\operatorname{grad}T)=|\vec{U}||\operatorname{grad}T|\cos\theta$, where θ is the intersection angle between velocity and temperature gradient. It is obvious that for a fixed flow rate and temperature difference, the smaller the intersection angle between the velocity and the temperature gradient, the larger the heat transfer rate. That is, the reduction of the intersection angle will increase the convective heat transfer. According to the Webster Dictionary [8], when several actions or forces are cooperative or combined, such situation can be called "synergy". Thus, this idea introduced for enhancing convective heat transfer focuses on the synergy

* Corresponding author. Tel.: +86-29-266-9106; fax: +86-29-323-7910.
E-mail address: wqtao@xjtu.edu.cn (W.-Q. Tao).

0017-9310/02/$ - see front matter © 2002 Published by Elsevier Science Ltd.
PII: S0017-9310(02)00097-2

Nomenclature

A	surface area, m^2
c_p	specific heat capacity, $J\,kg^{-1}\,K^{-1}$
H	duct height or transverse distance between plates, m
h	heat transfer coefficient, $W\,m^{-2}\,K^{-1}$
Int	integral, $\int_\Omega \rho c_p(\vec{U}\cdot \mathrm{grad}\,T)\,dA$, W
Int′	modified integral, $\int_\Omega(\vec{U}\cdot \mathrm{grad}\,T)\,dA$, $m^3\,K\,s^{-1}$
k	thermal conductivity, $W\,m^{-1}\,k^{-1}$
L	length, m
$\vec{n}$	outward normal unit vector
Nu	Nusselt number
q	heat flux, $W\,m^{-2}$
Re	Reynolds number
R	radius, m
S	length of arc, m
t	plate thickness, m
T	temperature
u, v	velocity component in x- and y-directions
$\vec{U}$	velocity vector
x, y	Cartesian coordinates, m
δ_t	thermal boundary layer thickness, m
θ	intersection angle between velocity and temperature gradient, degree
ρ	fluid density, $kg\,m^{-3}$
ϕ	oblique or inclined angle, degree

Subscripts

f	fluid
in	inlet
m	mean
max	maximum
min	minimum
w	wall

between velocity and temperature gradient and will be hereafter called "field synergy principle".

2. Extension of the field synergy principle to elliptic flow cases

Most convective heat transfer problems encountered in engineering are of elliptic type, and hence, extending the "field synergy principle" to elliptic cases will be of great importance.

Consider a typical elliptic convective heat transfer case—fluid flow and heat transfer over a backward step, as shown in Fig. 1. The solid walls are of constant temperature T_w, and fluid with temperature T_f flows into the domain. The 2-D energy equation for this case can be written as

$$\rho c_p\left(u\frac{\partial T}{\partial x}+v\frac{\partial T}{\partial y}\right)=\frac{\partial}{\partial x}\left(k\frac{\partial T}{\partial x}\right)+\frac{\partial}{\partial y}\left(k\frac{\partial T}{\partial y}\right) \tag{3}$$

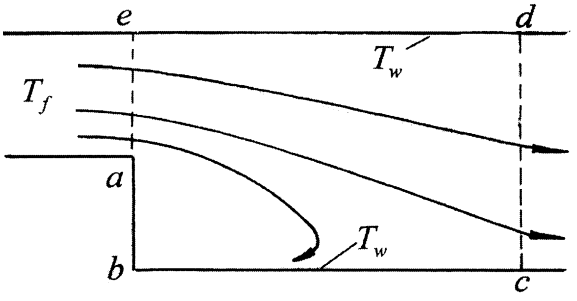

Fig. 1. Fluid flow and heat transfer over a backward step.

We now integrate this equation over the entire domain Ω_{abcdea}, and express the integral of the left and right parts by FM and HD, respectively, we have:

$$\mathrm{FM}=\int\int_\Omega \rho c_p(\vec{U}\cdot\nabla T)\,dx\,dy \tag{4a}$$

$$\mathrm{HD}=\int\int_\Omega\left[\frac{\partial}{\partial x}\left(k\frac{\partial T}{\partial x}\right)+\frac{\partial}{\partial y}\left(k\frac{\partial T}{\partial y}\right)\right]dx\,dy \tag{4b}$$

By using the Gauss theorem for reduction of the integral dimension, Eq. (4b) can be rewritten as

$$\begin{aligned}\mathrm{HD}&=\oint_{\partial\Omega_{abcdea}}\vec{n}\cdot k\nabla T\,dx\,dy\\&=\int_{abc}\vec{n}\cdot k\nabla T\,dS+\int_{cd}\vec{n}\cdot k\nabla T\,dS\\&\quad+\int_{de}\vec{n}\cdot k\nabla T\,dS+\int_{ea}\vec{n}\cdot k\nabla T\,dS\end{aligned} \tag{5}$$

where $\vec{n}$ represents the outward normal along each boundary, and dS is the length differential of boundary. Moving the integrals along the inlet and outlet boundaries of computation domain to the left hand of the balance equation, we have

$$\begin{aligned}&\int\int_{\Omega_{abcdea}}\rho c_p(\vec{U}\cdot\nabla T)\,dx\,dy-\int_{cd}\vec{n}\cdot k\nabla T\,dS\\&\quad-\int_{ea}\vec{n}\cdot k\nabla T\,dS=\int_{abc}\vec{n}\cdot k\nabla T\,dS+\int_{de}\vec{n}\cdot k\nabla T\,dS\end{aligned} \tag{6}$$

The right-hand side of Eq. (6) stands for the heat transfer between the surface of the backward step and the fluid, which is the convective heat transfer between

the fluid and the solid surface. The first term at the left-hand side is the energy transferred due to fluid motion, while the second and the third terms represent the axial heat conduction within the fluid. It is well known that [9], for fluids with a Peclet number greater than 100, the axial heat conduction within the fluids may be neglected compared to the energy transferred by the fluid motion. For conventional working fluids adopted in engineering, the Peclet numbers are usually greater than 100, and hence, the integration $\int\int_{\Omega} \rho c_p(\vec{U} \cdot \mathrm{grad}\, T)\,\mathrm{d}x\,\mathrm{d}y$ actually represents the energy transferred by convection. Thus it is clear that a better synergy (i.e., decreasing the intersection angle between the velocity vector and the temperature gradient) will make the integration $\int\int_{\Omega} \rho c_p(\vec{U} \cdot \mathrm{grad}\, T)\,\mathrm{d}x\,\mathrm{d}y$ larger, i.e., enhancing the heat transfer. Even for fluids whose Peclet number is less than 100, the reduction of the intersection angle between velocity and the temperature gradient can also enhance heat transfer, though the effect is not so significant as for the case with a larger Peclet number. Thus either for parabolic flow or for elliptic flows, the idea proposed in [6,7] is all valid. The extension of above discussion to three-dimensional case is very straightforward, and will not be discussed here for simplicity.

The contents mentioned above, is a rather new idea in the heat transfer literatures. It is better to have some verifications in order to give readers more confidence in this concept. We have conducted verifications, which can be grouped into two types: primary verification and advanced verification. For the primary verification, we check the integration over the entire domain to see if its variation trend with Reynolds number is the same as the averaged Nusselt number or heat transfer coefficient of the studied surface. The advanced verification means applying this principle to design heat transfer surface which can effectively enhance the convective heat transfer.

3. Primary verifications

For more than 10 heat transfer surfaces, numerical computations were carried out to obtain the integral of $\int\int_{\Omega} \rho c_p(\vec{U} \cdot \mathrm{grad}\, T)\,\mathrm{d}A$ over the whole computation domain and the average Nusselt number for the configuration studied. For the simplicity of presentation, the integral will be represented by "Int" and the numerical results of five cases are provided. All computations were conducted by finite volume method, with SIMPLE algorithm to deal with the linkage between velocity and pressure. The power-law scheme was used to discretize the convection and diffusion term. All the flows computed were assumed to be laminar and in steady state. For the first four cases the periodic fully developed convective heat transfer was simulated and the cyclic average Nusselt number was determined for the constant wall temperature case. For all the five examples, air was used as the heat transfer medium.

3.1. Heat transfer for fluid flowing across discrete parallel plates

The configuration studied is presented in Fig. 2. The computation conditions are as follows: $L_1 = L_2$, $H/L_1 = 0.6$, $H/t = 1.5$, $Pr = 0.707$. The grid number used was 44×22. For comparison purpose, the continuous parallel plate duct with width H was taken as the reference duct. The characteristic length for the Nusselt number and Reynolds number was taken as $2H$ for both cases.

The numerical results are shown in Figs. 3 and 4. The Nusselt number in the fully developed region will be 7.54 [10], and numerical result agrees with this very well (with a grid system of 44×26). Two features may be noted. First, the variation trends of Int and *Nu* with *Re* are very similar, and both Int and *Nu* of the discrete parallel plates are much higher than that of the continuous plate duct; second, the Nusselt number tends to be kept constant, independent of *Re* computed, while the value of Int decreases with decreasing in Reynolds number in the region for which heat conduction within the fluid

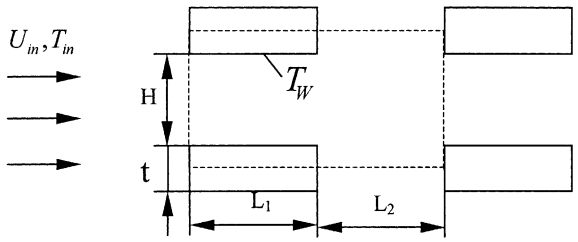

Fig. 2. Heat transfer across discrete parallel plates.

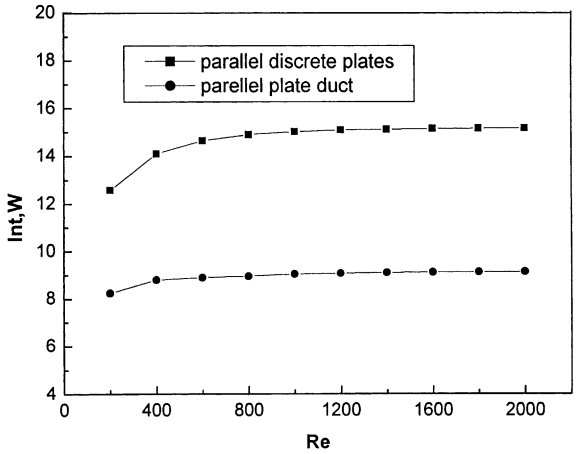

Fig. 3. The variation of Int with Reynolds number (flow across discrete parallel plates).

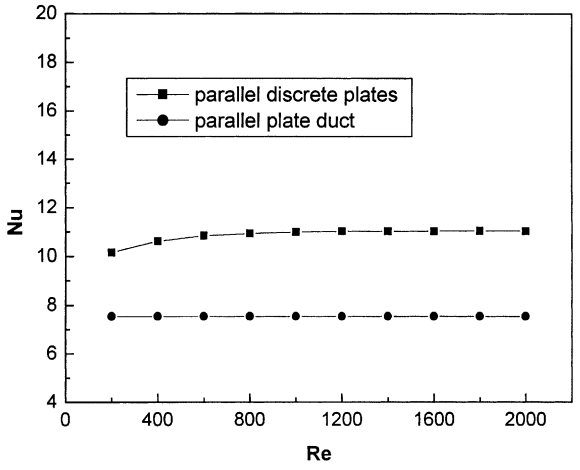

Fig. 4. The variation of *Nu* with Reynolds number (flow across discrete parallel plates).

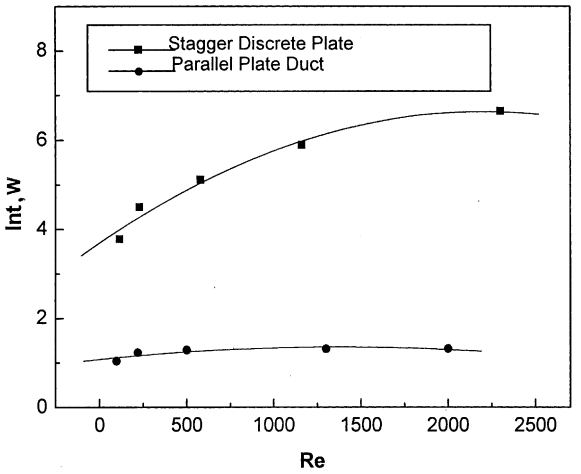

Fig. 6. The variation of *Nu* with Reynolds number (flow across discrete staggered plates).

plays a role and the percentage of heat transfer via fluid motion starts to decrease as *Re* decreases. Similar variation trends may be found in following examples.

3.2. Heat transfer for fluid flowing across discrete staggered plates

The configuration studied is presented in Fig. 5. The computation conditions are as follows: $L/H = 0.5$, $t/H = 1/3$, $Pr = 0.707$. A grid system of 50×29 was used, and the characteristic length of *Nu* and *Re* was taken as (*H*–*t*), which corresponds to the twice of the width between two adjacent plates.

The numerical results are shown in Figs. 6 and 7. Obviously, the variation trends of Int and *Nu* with *Re* are very similar to each other.

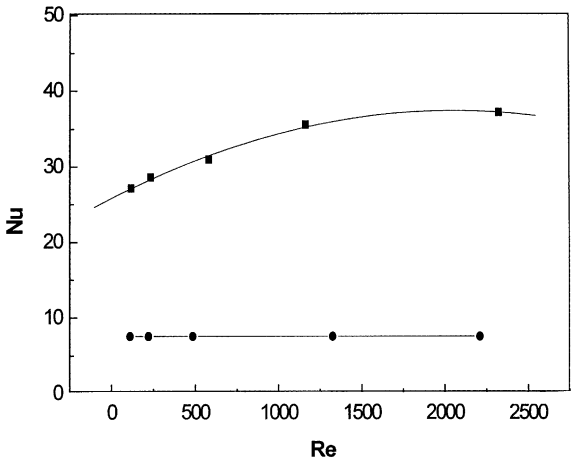

Fig. 7. The variation of Int with Reynolds number (flow across discrete staggered plates).

3.3. Heat transfer in a two-dimensional wavy channel

The configuration studied is presented in Fig. 8. Computations were conducted under following condi-

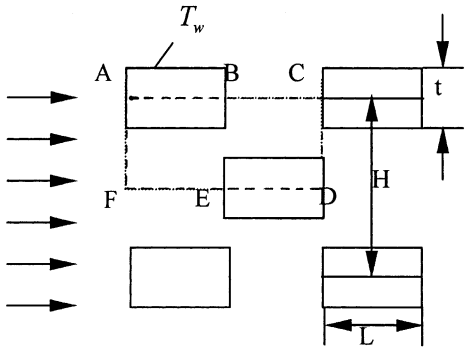

Fig. 5. Heat transfer across discrete staggered plates.

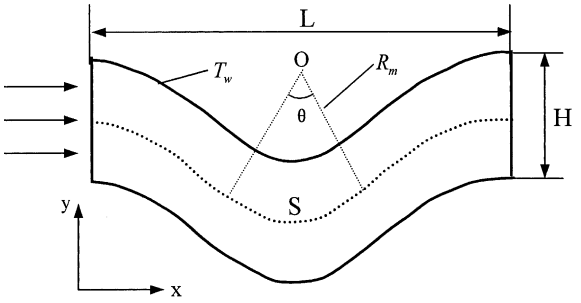

Fig. 8. Heat transfer in a wavy channel.

tions: $R_m/S = 0.6$, $L/S = 1.84$, $H/S = 0.6$, $Pr = 0.707$. The grid number user was 48×22, and $2H$ was taken as the characteristic length.

Numerical results presented in Figs. 9 and 10 indicate the same variation trend of Int vs. *Re* and *Nu* vs. *Re*.

3.4. Heat transfer in a corrugate duct

A diverging and converging duct is shown in Fig. 11. Following conditions were adopted in the computation: $H_{min}/L = 1/3$, $H_{max}/L = 2/3$, $Pr = 0.707$. A mesh of 42×42 was used. The characteristic length was taken as $(H_{min} + H_{max})/2$.

The numerical results presented in Figs. 12 and 13 obviously lead to the same conclusion presented before.

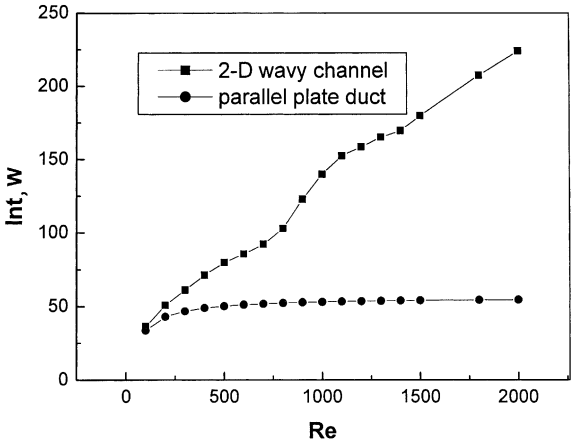

Fig. 9. The variation of Int with Reynolds number (flow in a wavy channel).

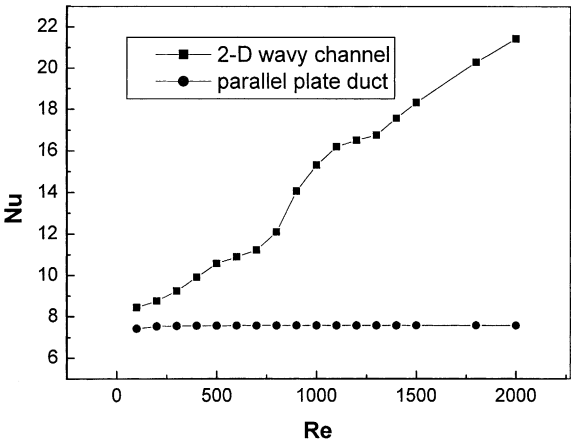

Fig. 10. The variation of *Nu* with Reynolds number (flow in a wavy channel).

3.5. Natural convection in square enclosure

Natural convection in square enclosure is a benchmark problem in computational heat transfer [11]. The two vertical walls of the enclosure are maintained at constant but different temperatures and the top and bottom walls are adiabatic. Our computations were conducted for *Ra* ranging from 10^3 to 10^6. The value of Nusselt number varies from about 1.1 to 8.8 [11]. To make a clear comparison between the variation trends of *Nu* and Int, a modified integral has been computed, which is defined as $\mathrm{Int}' = \mathrm{Int}/\rho c_p$. The variation range of the modified integral is from about 0 to 5, which is in the same order as Nusselt number. The curve of *Nu* vs. *Ra* was then lowered down such that at $Ra = 10^6$, the curve of *Nu* vs. *Ra* coincides with the curve of Int′ vs. *Ra*. The numerical results are presented in Fig. 14, from which the value of Int′ (and Int) for the entire domain is zero, since the heat released at hot surface is absorbed at the cold surface. The enclosure was vertically cut into two parts and integration was only conducted for one of the parts, with artificially cut boundary where the heat conduction within the fluids occurs. The dashed line in Fig. 14 represents the variation trend of Nusselt number of one vertical wall, while the solid line stands for the integral. It can be seen that in the low Rayleigh number region, the heat conduction within the fluid becomes important, and hence the difference between the value of Int′ and that of *Nu* gradually becomes larger and larger with the decreasing in *Ra*.

4. Applying field synergy principle to develop new heat transfer surfaces

Probably the most challenging task of developing the field synergy principle is to design enhanced heat transfer surfaces at the guidance of the principle. Such work is now underway in the authors' group. Some computational results are presented for illustration.

4.1. Heat transfer across plate array positioned obliquely to the flow direction

Plate array positioned obliquely to the oncoming flow is shown in Fig. 15. It may be regarded as a 2-D model for louver fin. The major geometric parameter affecting heat transfer performance is the oblique angle ϕ. Laminar fluid flow and heat transfer were simulated for the periodic fully developed situation with varying angle ϕ. The geometric parameters were set as $T_p/L = 1$, $L_p/L = 1$, $t/L = 1/15$. The grid numbers in *x*- and *y*-directions were 82 and 42, respectively.

Comparison of our numerical and experimental results presented in Figs. 16 and 17 shows the intersection angle variation trend. Both test data and simulation

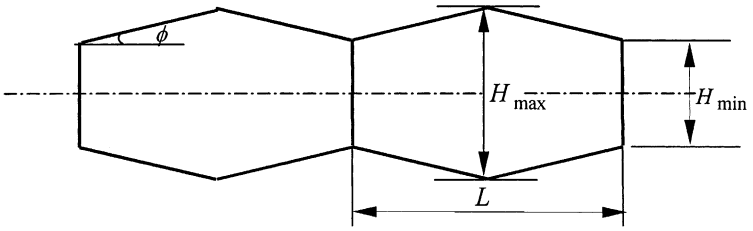

Fig. 11. Corrugate duct.

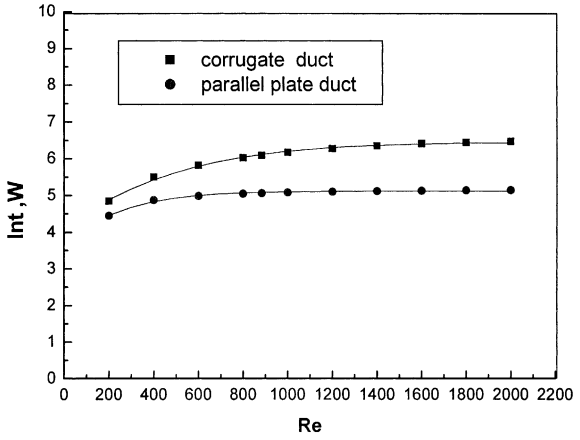

Fig. 12. The variation of Int with Reynolds number (flow in a corrugate duct).

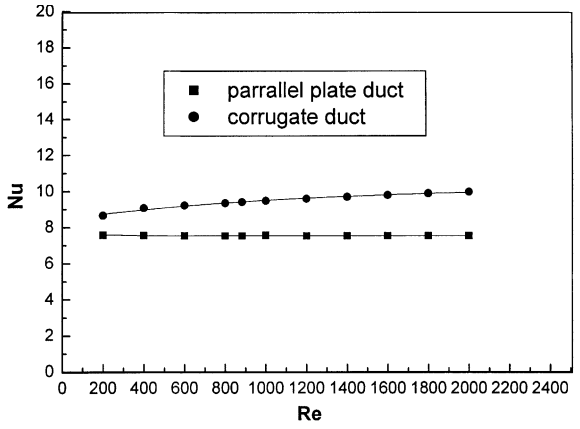

Fig. 13. The variation of *Nu* with Reynolds number (flow in a corrugate duct).

results show that Nusselt number reaches its maximum for $\phi \approx 30°$, and Fig. 17 shows that at this oblique angle the average intersection angle correspondingly reaches its minimum, exactly indicating the synergy concept.

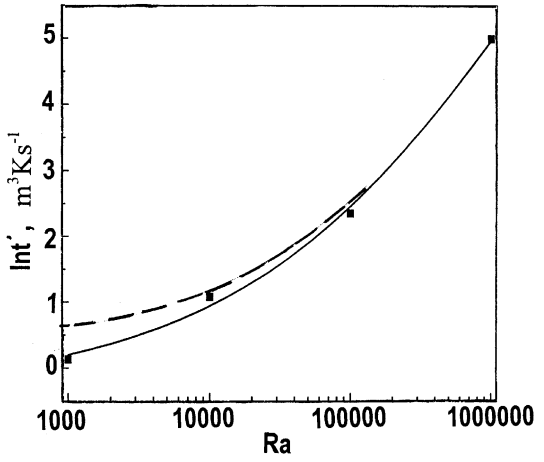

Fig. 14. *Nu* vs. *Ra* and Int′ vs. *Ra* for natural convection in square enclosure.

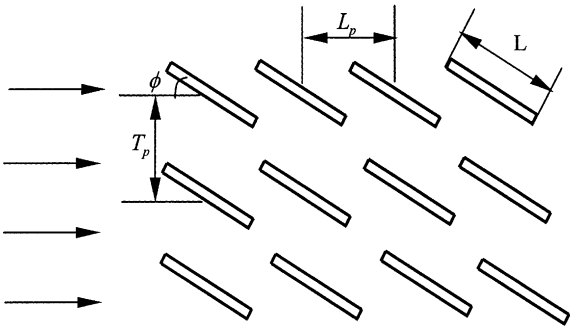

Fig. 15. Obliquely-positioned plate array.

4.2. Heat transfer in a corrugate duct

The effect of the inclined angle of the corrugate duct wall, ϕ, shown in Fig. 11, was investigated for the periodic fully developed situation. A grid system of 42×42 was used. The variation of inclined angle was implemented by varying the value of H_{max}, while keeping L and H_{min} unchanged. The relation between the cycle average heat transfer coefficient with the inclined angle is

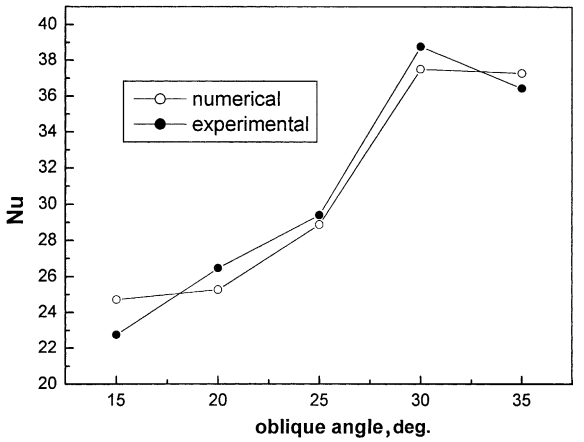

Fig. 16. Nusselt number vs. oblique angle.

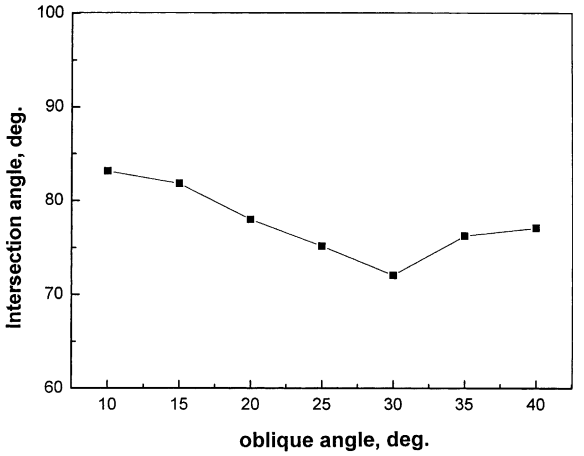

Fig. 17. Average intersection angle vs. oblique angle.

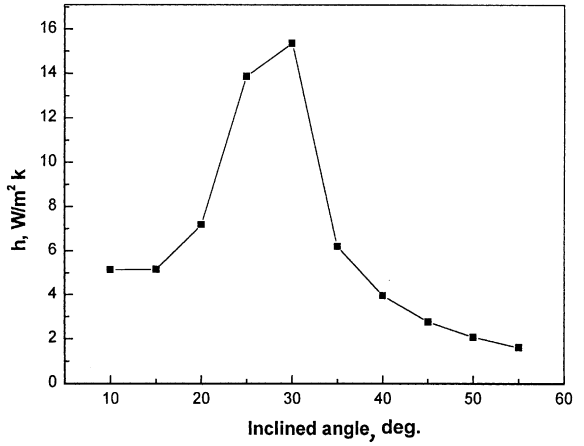

Fig. 18. Average Nusselt number vs. inclined angle of corrugate duct.

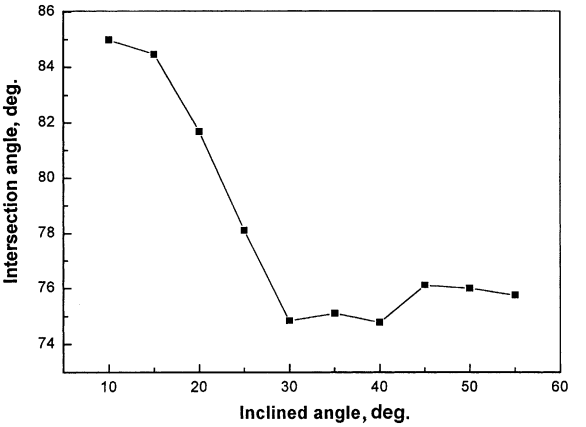

Fig. 19. Average intersection angle vs. inclined angle of corrugate duct.

presented in Fig. 18 and the curve of θ_m vs. ϕ is presented in Fig. 19. The numerical results demonstrate once again that the configuration with highest heat transfer rate has the minimum average intersection angle between velocity and temperature gradient.

The two examples mentioned above show that the best performance of an enhanced heat transfer surface may be reached if the geometric parameter(s) of the configuration could make the average intersection angle minimum. This gives us a guidance to reveal the best geometric parameters in developing an enhanced heat transfer surface.

5. Conclusions

In this paper, the new concept "field synergy principle" proposed firstly in [6,7] is extended from parabolic flow to elliptic flow. According to this principle, the convective heat transfer can be enhanced by reducing the intersection angle between the velocity and the temperature gradient. Several numerical examples are provided to show the validity of the principle.

Acknowledgements

This work was supported by the National Fundamental R&D Project of China (Grant number 2000026303). The authors are grateful to Mr. Z.G. Qu, X. Liu, F.Q. Song, Ms. X. Wang, and M.X. Li, for carrying out some numerical computations.

References

[1] A.E. Bergles, Heat transfer enhancement—the maturing of the second-generation heat transfer technology, Heat Transfer Engineering 18 (1997) 47–55.

[2] A.E. Bergles, Heat transfer enhancement—the encouragement and accommodation of high heat fluxes, ASME J. Heat Transfer 119 (1997) 8–19.
[3] A.E. Bergles, Techniques to enhance heat transfer, in: W.M. Rohsenow, J.P. Hartnett, Y.I. Chi (Eds.), Handbook of Heat Transfer, third ed., McGraw-Hill, New York, 1998, pp. 11.1–11.76.
[4] A.E. Bergles, Enhanced heat transfer: endless frontier, or mature and routine? Enhanced Heat Transfer 6 (1999) 79–88.
[5] R.L. Webb, in: Principles of Enhanced Heat Transfer, John Wiley & Sons Inc., New York, 1994, p. 89.
[6] Z.Y. Guo, D.Y. Li, B.X. Wang, A novel concept for convective heat transfer enhancement, Int. J. Heat Mass Transfer 41 (1998) 2221–2225.
[7] S. Wang, Z.X. Li, Z.Y. Guo, Novel concept and device of heat transfer augmentation, in: Proceedings of 11th IHTC, vol. 5, 1998, pp. 405–408.
[8] D.B Guralnik, editor-in-chief, WEBSTER'S New World Dictionary of the American Language, Second College Edition. William Collins Publishers, Inc. Cleveland, 1979, p. 1444.
[9] W.M. Kays, M.E. Crawford, in: Convective Heat and Mass Transfer, McGraw-Hill Book Company, New York, 1980, p. 107,246.
[10] F.P. Incropera, D.P. DeWitt, in: Introduction to Heat Transfer, third ed., John Wiley & Sons, New York, 1996, p. 396.
[11] W.Q. Tao, Numerical Heat Transfer (in Chinese), second ed., Xi'an Jiaotong University Press, Xi'an China, 2001.